

NJC

Accepted Manuscript



This article can be cited before page numbers have been issued, to do this please use: A. Heydari-turkmani, S. Zakavi and N. Nikfarjam, *New J. Chem.*, 2017, DOI: 10.1039/C7NJ00791D.



This is an Accepted Manuscript, which has been through the Royal Society of Chemistry peer review process and has been accepted for publication.

Accepted Manuscripts are published online shortly after acceptance, before technical editing, formatting and proof reading. Using this free service, authors can make their results available to the community, in citable form, before we publish the edited article. We will replace this Accepted Manuscript with the edited and formatted Advance Article as soon as it is available.

You can find more information about Accepted Manuscripts in the [author guidelines](#).

Please note that technical editing may introduce minor changes to the text and/or graphics, which may alter content. The journal's standard [Terms & Conditions](#) and the ethical guidelines, outlined in our [author and reviewer resource centre](#), still apply. In no event shall the Royal Society of Chemistry be held responsible for any errors or omissions in this Accepted Manuscript or any consequences arising from the use of any information it contains.



Journal Name

ARTICLE

Novel metal free porphyrinic photosensitizers supported on solvent-induced Amberlyst-15 nanoparticles with a porous structure

Akram Heydari-turkmani, Saeed Zakavi* and Nasser Nikfarjam*

Received 00th January 20xx,
Accepted 00th January 20xx

DOI: 10.1039/x0xx00000x

www.rsc.org/

In this study, a series of meso-tetraarylporphyrins (aryl = phenyl, 2-methylphenyl and 2-chlorophenyl), H₂T(aryl)P immobilized on nanosized Amberlyst-15 (nanoAmb) through acid-base reaction were utilized as highly efficient (turnover number in the range of 4 × (8000 to 10000), for 4 successive reactions with the same catalyst), stable and reusable heterogeneous photocatalysts for the aerobic oxidation of olefins under green conditions. Interestingly, nanoAmb with an average diameter less than 200 nm was produced from Amb beads by overnight magnetic stirring in ethyl acetate at room temperature. The catalysts may be reused at least four times without significant decrease in the catalytic activity. The immobilization of porphyrin on the polymer was confirmed by diffuse reflectance UV-vis and IR spectroscopy. Also, the supported porphyrin was released from nanoAmb surface by alkaline treatment and analyzed by UV-vis spectroscopy. N₂ porosimetry analysis showed significant decreased BET surface area and pore volume values of the polymer after the immobilization of porphyrins. The influence of different parameters including the photosensitizer to olefin molar ratio, porphyrin loading, solvent, type of light source and the meso substituents has been investigated. H₂T(2-Me)PP@nanoAmb and H₂T(2-Cl)PP@nanoAmb showed the highest oxidative stability and catalytic activity among the series of porphyrins, respectively. In order to overcome the photooxidative degradation of porphyrin photosensitizers, different degrees of catalyst loading were examined and that with the lowest loading showed the best performance. The use of 1,4-benzoquinone and 1,3-diphenylisobenzofuran as the quencher of superoxide anion radical and singlet oxygen species revealed that oxidation reaction mainly proceeds with a singlet oxygen mechanism.

Introduction

Porphyrins, porphyrinoids and their metal complexes have been used extensively as photosensitizers in synthetic chemistry as well as environmental and medical applications^[1-6]. Over the past decades, much attention was paid to design new photosensitizers with the aim of improving the efficiency of production of reactive oxygen species (ROS) and especially singlet oxygen^[7-12]. Porphyrins may be readily protonated with different weak and strong acids^[13-15]. However, little attention was paid to porphyrin diprotonated species as potential photosensitizers with red-shifted absorption bands in the visible region. In spite of some advantages of homogeneous

catalysts over their heterogeneous counterparts such as higher catalytic activity, heterogenizing homogeneous catalysts is an efficient approach to overcome problems encountered with the use of the former including difficulties in separation and recovery as well as the oxidative degradation of the catalyst. Different organic and inorganic supports may be employed to immobilize the porphyrin based catalysts^[2, 16-19]. In the case of metalloporphyrins, functionalization of the organic and inorganic supports with efficient nitrogen donors such as imidazole may be used for this purpose^[20-22]. Also, the introduction of anionic and cationic centres on the support has been utilized to immobilize porphyrins and metalloporphyrins with cationic and anionic substituents, respectively^[23-24]. The lack of metal centre in the case of free base porphyrins necessitates the introduction of different anionic and cationic groups at the periphery of porphyrin core. Accordingly, supports bearing weak and strong acidic substituents may be used as simple supports to immobilize a wide range of porphyrins with no special peripheral substituents^[25-26]. Indeed, core protonation of porphyrins may be used as a low-

^a Department of Chemistry, Institute for Advanced Studies in Basic Sciences (IASBS), Zanjan 45137-66731, Iran. E-mail: zakavi@iasbs.ac.ir

† Footnotes relating to the title and/or authors should appear here. Electronic Supplementary Information (ESI) available: [details of any supplementary information available should be included here]. See DOI: 10.1039/x0xx00000x

cost alternative of complex multi-step procedures have been used to functionalize porphyrins at the β and meso positions [27]. Furthermore, the structural and electronic changes upon the protonation of porphyrins such as the out-of-plane deformation of porphyrin core and decreased dihedral angle between the porphyrin mean plane and the meso aryl substituents lead to significant difference between porphyrins [13, 28]. It should be noted that in free base meso-tetraarylporphyrins, in the absence of remarkable steric hindrance between the meso aryl groups and the β carbon atoms, there are large dihedral angles between the aryl substituents and porphyrin mean plane [29]. This in turn leads to little or no difference between the structure and electronic properties of porphyrins with various electron releasing and with-drawing substituents. Amberlyst 15 dry (Amb) is a bead form, strongly acidic ion exchange resin that has been used as acidic catalyst in different organic transformations [10, 30, 31]. This polymer is cheap, non-toxic and environmentally compatible. Also, the stability of Amb towards degradation under oxidative conditions makes it suitable for using as support for immobilization of oxidation catalysts [10]. In spite of the extensive studies performed on the spectral and structural properties of porphyrin dications, to date, little attention has been paid to the effects of core protonation on the photocatalytic activity of porphyrin photosensitizers [32-33].

Indeed, the formation of porphyrin diacids was considered as an undesired side reaction during the use of porphyrin free base photosensitizers in chlorinated solvents [34]. In 2015, oxidation of artemisinin catalyzed by an Amb supported porphyrin in liquid CO_2 was reported by George et al. [32]. In another study, the influence of UV light on the photostability of some porphyrin diacids with CH_3COOH was investigated [33]. In the present study, Amberlyst 15 nanoparticles (nanoAmb) prepared by stirring the polymer beads in diethyl acetate at room temperature was utilized as a strong acid to protonate a series of meso-tetraarylporphyrins (Figure 1). Also, due to the insolubility of the polymer in the solvent used in this study, the diprotonated species were immobilized electrostatically on the anionic polymer. It is noteworthy that the deprotonated polymer acts as the counteranion of the diprotonated species and therefore in the absence of alkaline agents, the diprotonated species is strongly bonded to the surface of the polymer and therefore no catalyst leaching has been observed. The nanoAmb supported porphyrins were used as photosensitizer for the aerobic oxidation of olefins in acetonitrile. The effects of parameters such as the mesosubstituents, light source, solvent and degree of porphyrin loading on the photocatalytic activity and oxidative stability of porphyrin diacids were investigated. Interestingly, turnover numbers as high as ca. 10000 were achieved for the oxidation reaction catalyzed by the diacids.

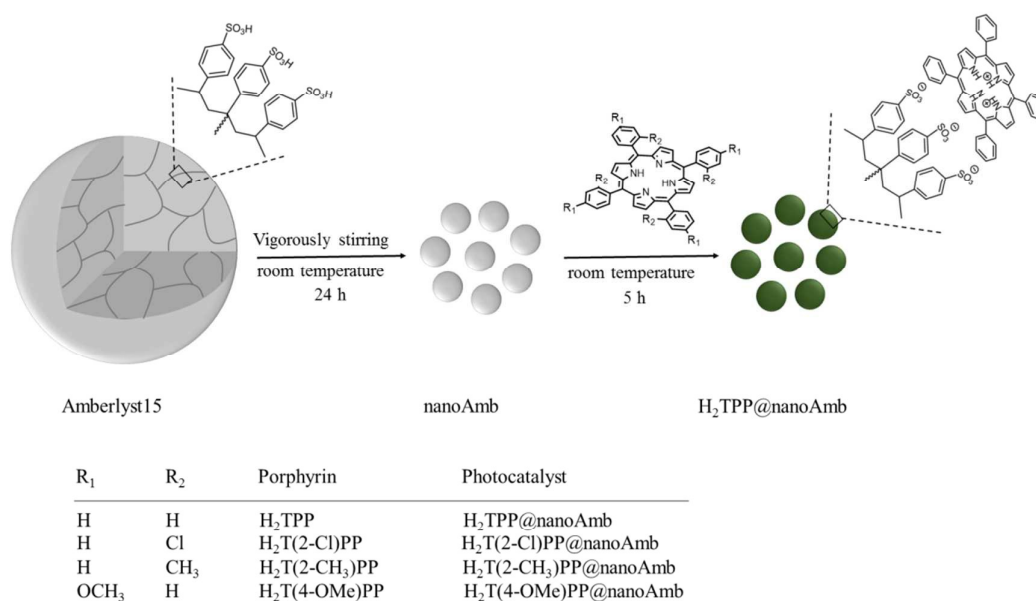


Figure 1. Schematic presentation of immobilization of porphyrins on Amberlyst 15 nanoparticles (nanoAmb).

Experimental**Instrumental**

A Pharmacia Biotech Ultrospec 4000 UV-Vis spectrophotometer was used for UV-vis spectroscopy. Diffuse reflectance UV-vis spectra were recorded using a Varian Cary 5000 UV-VIS-NIR absorption spectrometer. ^1H NMR spectra were obtained on a BrukerAvance DPX-400MHz spectrometer. The reaction mixtures were analyzed by a Varian-3800 gas chromatograph equipped with a HP-5 capillary column and flame-ionization detector. The oxidation products were characterized by ^{13}C NMR. DR-FT-IR spectra were prepared with a Bruker Vector 22 instrument after mixing the samples with KBr. The porosimetry analyses were performed by nitrogen adsorption/desorption method using a Belsorp max (Japan) instrument. The mean diameter and size distribution of the aqueous dispersion of particles before and after loading of porphyrin were measured by Zetasizer Nano ZS (Malvern Instruments Ltd., United Kingdom). All measurements were performed at 25°C with an angle detection of 90° . The sample was previously filtered with a $0.45\ \mu\text{m}$ Millipore filter to avoid any contamination. For morphology investigation by the field-emission scanning electron microscopy (FE-SEM), the crushed Amberlyst beads obtained after 5 and 24 h were set on a clean glass slide and then vacuum-coated with gold. Digital images of the samples were acquired with the HitachiS4160 field emission scanning electron microscope operating at 20 kV.

Synthesis and characterization of H_2TPP , $\text{H}_2\text{T}(2\text{-Cl})\text{PP}$, $\text{H}_2\text{T}(2\text{-Me})\text{PP}$ and $\text{H}_2\text{T}(4\text{-OMe})\text{PP}@$ nanoAmb

Meso-tetraphenylporphyrin H_2TPP and its derivatives with para-methoxy, $\text{H}_2\text{T}(4\text{-OMe})\text{PP}$, ortho-methyl, $\text{H}_2\text{T}(2\text{-Me})\text{PP}$ and 2-chloro, $\text{H}_2\text{T}(2\text{-Cl})\text{PP}$ [35] were synthesized, characterized and purified according to the literature methods. The ^1H NMR, ^{13}C NMR and UV-Vis spectral data of the porphyrins are presented in the Supporting Information, S1. Amberlyst 15 beads (dry, Acros) were stirred vigorously over a magnetic stirrer in ethyl acetate overnight at room temperature to obtain the pale yellow powder of nanoAmb. A solution of the desired porphyrin (0.08 mmol) in 25 ml ethyl acetate was added to 1.5 g nanoAmb and the mixture was stirred for 5 h at room temperature in air. After the required time, the pale yellow nanoAmb turned to green. The solid was separated by centrifuging and was washed two times with ethyl acetate. The loaded porphyrin was measured by UV-vis spectroscopy; Tetra-n-butylammonium hydroxide was added to the mobilized porphyrin in ethyl acetate to release the acid bonded porphyrin. The released porphyrin was measured by absorbance measurement at the λ_{max} of each porphyrin.

General oxidation procedure

The photooxidation reactions were performed in a double walled cylindrical glass vessel (Supporting Information, Figure S1). Water circulation through the outer jacket was used to maintain a constant temperature. In a typical reaction, 6.6×10^{-4} mmol photosensitizer and olefin (0.66 to 6.6 mmol) were

added to 10 ml acetonitrile to obtain the desired molar ratio. At different time intervals, an aliquot of the solution was taken out with a syringe and analyzed by GC. In order to characterize the oxidation products, a control reaction was performed in CDCl_3 under the same conditions. The ^{13}C NMR spectrum confirmed the formation of cyclooct-1-en-3-yl hydroperoxide and 2-cyclohexene-1-one in the oxidation of cyclooctene and cyclohexene, respectively. The spectral data of the products are summarized in the in the (Supporting Information, S2 and S3).

Results and discussion

Amb nanoparticles were prepared by magnetically stirring overnight Amberlyst 15 beads in diethyl acetate. Interestingly, the beads break down into small particles over time (Figure 2, A, B, C and D).

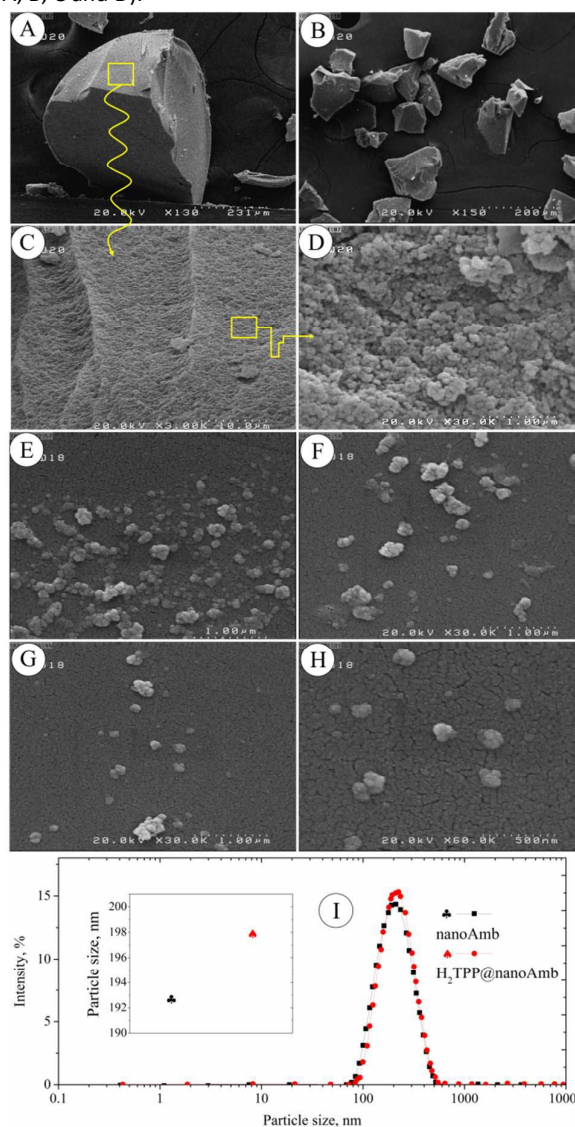


Figure 2. FE-SEM images indicating the structural changes upon magnetic stirring of Amb in ethyl acetate up to 24 h. DLS characterization of Amb nanoparticles and $\text{H}_2\text{TPP}@$ nanoAmb.

ARTICLE

Journal Name

The results of dynamic light scattering (DLS) confirmed the formation of polymer nanoparticles with an average diameter of 192 nm. Field-emission scanning electron microscopy (FE-SEM) images revealed the formation of nearly spherical nanoparticles with an average diameter of less than 200 nm. Also, DLS showed an average diameter of 198 nm for the porphyrin supported polymer (Figure 2, I). Diffuse reflectance UV-vis spectra of the catalysts (Figure 3) showed the presence of porphyrins on the polymer support. The red shift of the Soret and Q(0,0) bands is in accord with the formation of porphyrin diprotonated species^[27,36]. It is noteworthy that the order of Soret and Q(0,0) band of different porphyrins in DR UV-Vis spectra correlates with that previously observed for the corresponding diacids in dichloromethane.^[13,36] The immobilization of porphyrins on the polymer was also studied by IR spectroscopy. The IR spectra of Amb, H₂TPP and H₂TPP@nanoAmb are shown in the Supporting Information, Figure S2. Upon the formation of porphyrin diacids the region of greatest difference is 1100-1500 cm⁻¹ that has been attributed to the stretching and bending modes of the pyrrole rings. It was shown by Stone et al. that the band due to the C-N stretching at ca. 1350 cm⁻¹ is almost absent in porphyrin diacid^[14]. However, the existence of strong bands due to the polymer support in this region made it impossible to observe the expected changes. Immobilization of H₂TPP on the polymer is accompanied with the protonation of the porphyrin core and the formation of strong intermolecular hydrogen bonds between the N-H groups and the counteranion of the acid. As may be seen from in the Supporting Information, Figure S2 the main difference between the IR spectra is the disappearance of the N-H stretch band at 3300 cm⁻¹. Apparently, the formation of strong hydrogen bonds between the -SO₃⁻ groups of Amb and [H₄TPP]²⁺ led to the broadness of the N-H stretch band and disappearance of this band. Amb is a macroporous resin^[37-38] and therefore the incorporation of porphyrins into the macropores is expected to decrease the porosity of the polymer.

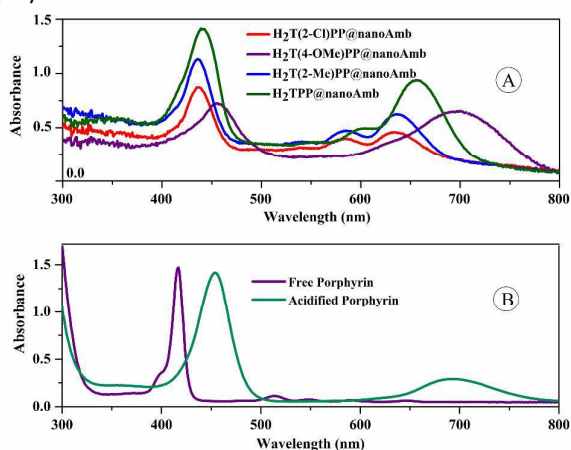


Figure 3 (a) Typical UV-vis spectrum of free base porphyrin (purple curve, H₂TPP) and its dication with sulfuric acid (green curve) in ethyl acetate; (b) Diffuse reflectance UV-vis spectra of the Amb immobilized porphyrins.

The nitrogen sorption isotherms of the solid catalysts are shown in (Figure 4). The isotherms are in accord with the macroporous structure of the catalysts^[39-40]. Also, the V_{total} and S_{BET} values, summarized in Table 1 show significant decreased BET surface area and pore volume values of the polymer after the immobilization of the porphyrins.

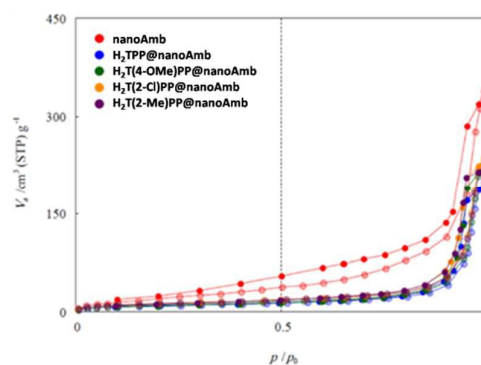


Figure 4. N₂ adsorption/desorption isotherms of nanoAmb and the immobilized porphyrins.

Oxidation of cyclooctene

The photooxidation of cyclooctene in the presence of the immobilized catalysts was studied and the influence of different factors was investigated.

Effect of catalyst:substrate molar ratio

In order to optimize the reaction conditions, the oxidation of cyclooctene in the presence of H₂TPP@nanoAmb in CH₃CN was studied. The degree of H₂TPP loading on Amb 15 was found to have significant influence on the catalytic activity of the catalyst (Table 2). It is observed that the maximum conversion was obtained using H₂TPP@nanoAmb with a loading of 0.003 mmol g⁻¹. This observation seems to be due to immobilization of H₂TPP at the outer surface of the polymer. It is noteworthy that H₂TPP@nanoAmb with this loading has the minimum amount of H₂TPP per gram of the polymeric support.

Table 1 BET analysis of Amb and the immobilized catalysts.

Entry	Photosensitizer	S_{BET}^a m ² g ⁻¹	V_t^b cm ³ g ⁻¹
1	Amb	85.0	0.5183
2	H ₂ TPP@nanoAmb	33.0	0.3000
3	H ₂ T(4-OMe)PP@nanoAmb	44.2	0.3422
4	H ₂ T(2-Cl)PP@nanoAmb	45.0	0.3600
5	H ₂ T(2-Me)PP@nanoAmb	37.8	0.3532

S_{BET}^a and V_t^b are specific surface area and total pore volume, respectively.

Table 2 Effect of the degree of porphyrin loading on photocatalytic activity of H₂TPP@Amb for the oxidation of cyclooctene in acetonitrile.^a

Catalyst	Porphyrin uptake/(mmol g ⁻¹) ^b	Catalyst weight (g)	H ₂ TPP Capacity (μmol)	Conversion (%) ^c	Oxidative Stability (%) ^d	TON ^e [TOF (h ⁻¹)] ^f
H ₂ TPP@nanoAmb	0.029	0.0227	0.668	58	40	5800[120]
H ₂ TPP@nanoAmb	0.024	0.0270	0.668	71	42	7100 [147]
H ₂ TPP@nanoAmb	0.019	0.0320	0.668	81	33	8100 [168]
H ₂ TPP@nanoAmb	0.009	0.0710	0.668	83	33	8300 [172]
H ₂ TPP@nanoAmb	0.003	0.2270	0.668	85	35	8500 [177]
nanoAmb	0	0.200	0	0	g	0

^a The supported H₂TPP and cyclooctene were used in 1:5000 molar ratio. ^b Evaluated by absorbance measurement at the λ_{max} of H₂TPP by UV-vis spectroscopy (see the text). ^c GC yield; the product was characterized by ¹³C NMR (Supporting Information, S2). ^d Measured on the basis of the absorbance changes at the λ_{max} of the released porphyrin after treatment with tetra-n-butylammonium hydroxide. ^eTON demonstrates the number of moles of product obtained per one mole of the catalyst. ^fTOF was obtained as turnover number of the reaction per time unit. ^g No oxidative degradation was detected.

On the other hand, due to the high molar ratio of photosensitizer to cyclooctene, i.e., 1:5000, there is no meaningful difference between the oxidative stability of the catalysts with different degrees of loading. BET analysis showed a porous structure for H₂TPP@nanoAmb. Also, this technique demonstrates a remarkable decrease in BET surface area of H₂TPP@nanoAmb with respect to that of Amb. Accordingly, the macropores of the polymer are occupied with H₂TPP. Apparently, the use of lower degrees of H₂TPP loading led to an increase in the number of catalytic sites at the surface of the heterogeneous catalyst. In other words, the catalytic sites at the surface of the polymer are more important in the oxidation reaction than those in the macropores. Furthermore, the molar ratio of catalyst to olefin was optimized (Table 3) and the 1:10000 one was found to be the best one.

Solvent effect

To optimize the solvent, the solvent, the oxidation of cyclooctene was conducted in different solvents (Table 4) and the highest conversion was obtained in acetonitrile. Also, the highest oxidative stability of the photosensitizer was observed in toluene.

The lifetime of singlet oxygen (τ) depends on the solvent^[41]. However, different values were reported for lifetime of singlet oxygen in a given solvent in the literature^[42] and therefore there is no certainty in the relative lifetime of this species in a series of solvent. The lifetime of singlet oxygen decreases as CH₃CN (77 μs) > DCE (63 μs) > Toluene (29 μs) > DMSO (19 μs) > DMF (17.9 μs) in the used solvents^[43]. The order of conversions approximately correlates with the order of lifetime of singlet oxygen in these solvents. As may be observed in Table 4, the oxidative stability of the catalyst in the used solvents decreases as Toluene > CH₃CN >> DCE > DMSO = DMF. It should be noted that mechanistic studies (*vide infra*) showed the involvement of singlet oxygen as the main reactive oxygen species. Furthermore, no product was obtained for the reactions performed in DMSO and DMF. It is noteworthy that these solvents are considered as singlet oxygen quencher^[44].

Effect of the light source

The type of light source is among the parameters influencing the photocatalytic activity of porphyrin-based photosensitizers^[45].

Table 3 Effect of catalyst to substrate molar ratio on the oxidation of cyclooctene in acetonitrile.^{a,b}

Catalyst:Substrate	Conversion (%)	Oxidative Stability (%)	TON [TOF (h ⁻¹)]
1:1000	35	----	350 [7]
1:5000	85	35	4250 [88]
1:10000 ^c	93	40	9300 [194]
1:15000	84	34	12600 [262]
1:20000	82	32	16400 [342]

^aH₂TPP@nanoAmber with a loading of 0.003 (Table 2) was used as catalyst. ^bThe reactions were conducted at room temperature. ^cThe optimum molar ratio.

Table 4 Solvent effect on the rate of reaction and the catalyst stability.^a

Entry	Solvent	Conversion (%)	Oxidative Stability (%) ^b
1	Acetonitrile	93	40
2	Toluene	11	78
3	1,2-Dichloroethane	73	8
4	Dimethylsulfoxide	Trace	0
5	Dimethylformamide	Trace	0

^a See the footnotes of Tables 2 and 3.

The oxidation of cyclooctene catalyzed by H₂TPP@nanoAmb was studied in the presence of different 20 W LED lamps (Figure 5 and Table 5) in CH₃CN. The results showed higher efficiency of the blue lamp compared to the red one. Accordingly, the absorption at the wavelength of the Soret band seems to be mainly responsible for the photosensitizer ability of the catalyst. Also, the white LED lamp was better than the other lamps. The conducting of the oxidation reaction in the presence of the Sun light led to very similar results to those with white LED lamp. Furthermore, the effect of light source on the oxidation reaction catalyzed by the other photosensitizers was studied and similar results were obtained (Table 5). It should be noted that as was expected the oxidative degradation of catalysts was greater in the presence of the blue LED lamp. In other words, the increase of the efficiency of singlet oxygen production led to both increase in the conversion of cyclooctene to the oxidative products and the oxidation of catalyst precursor.

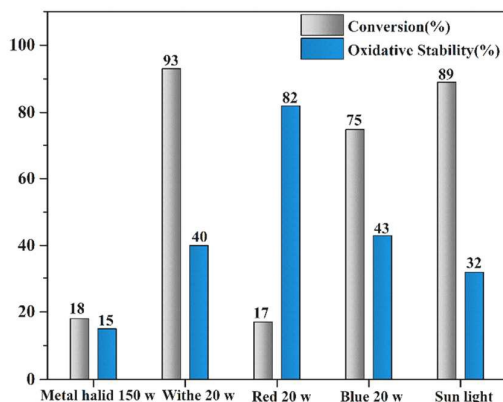


Figure 5. Effect of the light source on the photocatalytic activity of $H_2TPP@nanoAmb$ for the oxidation of cyclooctene in acetonitrile.

Effect of the meso substituents

The catalytic activity of different nanoAmb supported porphyrins was studied (Table 5 and Figure 6). It is observed that the catalytic activity decreased as $H_2T(2-Cl)PP@nanoAmb \geq H_2T(2-Me)PP@nanoAmb > H_2TPP@nanoAmb \gg H_2T(4-OMe)PP@nanoAmb$. Also, the oxidative stability of the photosensitizer was in the order of $H_2T(2-Me)PP@nanoAmb > H_2T(2-Cl)PP@nanoAmb > H_2TPP@nanoAmb \gg H_2T(4-OMe)PP@nanoAmb$. Accordingly, the electron deficient porphyrins were more efficient than the electron-rich ones. Also, the oxidative stability of the photosensitizers approximately correlates with the degree of electron deficiency of the porphyrins. However, higher oxidative stability of $H_2T(2-Me)PP@nanoAmb$ cannot be explained by the electronic properties of the ortho substituents. Apparently, the greater size of methyl (200 pm) group relative to chlorine atom (175 pm)^[46], led to increased steric hindrance at the meso position of the former and led to the observed order of oxidative stability.

Table 5 Photocatalytic activity of the catalysts in the presence of different light sources.^a

Photosensitizer	Time (h)	Conversion (Oxidative stability) (%)			
		White LED (20 w)	Blue LED (20 w)	Red LED (20 w)	Sun Light
$H_2TPP@Amb$	48	93(40)	43(38)	17(84)	89(32)
$H_2T(2-Cl)PP@Amb^b$	24	87(49)	58(59)	9(88)	92(44)
$H_2T(2-Me)PP@Amb^b$	24	82(83)	91(29)	7(93)	89(76)

^a Reactions were performed using the catalyst and cyclooctene in 1:10000 molar ratio.

^b The loading of porphyrin was 0.003 mmol.g⁻¹ (see Table 2).

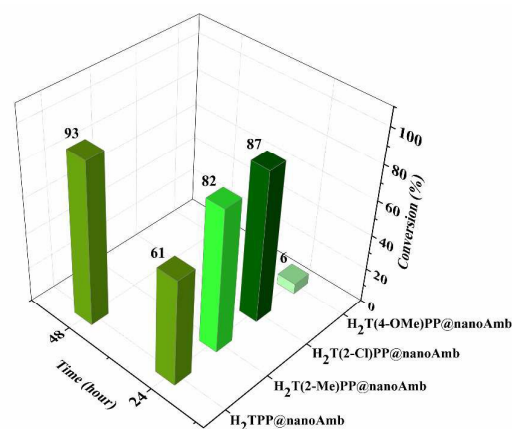


Figure 6. Photocatalytic activity of nano-Amb immobilized porphyrins with different meso substituents under the optimized conditions.

catalyst reusability

One advantage of heterogeneous catalysts over their homogeneous counterparts is their reusability. For the catalysts high stability of the catalyst under oxidative conditions facilitates the reuse of catalyst. The reusability of the catalysts was examined for four successive reactions (Figure 7). It is observed that the catalysts may be reused at least four times without significant decrease in the catalytic activity. However, after the fourth run, the catalyst degradation was significant in the case of $H_2TPP@nanoAmb$ and $H_2T(2-Cl)PP@nanoAmb$. In the case of $H_2T(2-Me)PP@nanoAmb$, ca. 66% of the catalyst was recovered after the fourth run. Accordingly, the latter is the best catalyst of the series on the basis of both catalyst stability and activity. It should be noted that while the reactions catalyzed by $H_2T(2-Cl)PP@nanoAmb$ and $H_2T(2-Me)PP@nanoAmb$ were performed in 24 h, the data demonstrated in Figures 7 and 8 for $H_2TPP@nanoAmb$ are for a reaction time of 48 h. The leaching of catalyst from the support surface is considered as a major problem associated with the use of immobilized catalysts. In the case of the nanoAmb supported porphyrins, only the presence of strong acids in the reaction media can leach the catalyst from the polymer surface. In other words, the formation of porphyrin diprotonated species with acids other than the $-SO_3H$ groups of the support should be avoided to prevent the leaching of porphyrins from the support surface. It is noteworthy that conducting of the photooxidation reactions in the presence of free base porphyrins in chlorinated solvents is associated with partial or complete protonation of porphyrins. In a control reaction, $H_2TPP@nanoAmb$ in DCE was treated with acidified DCE for 1 h. After 1 h, the mixture was filtered and the UV-vis spectrum of the DCE solution was prepared. Interestingly, the UV-vis spectrum showed no porphyrin dication.

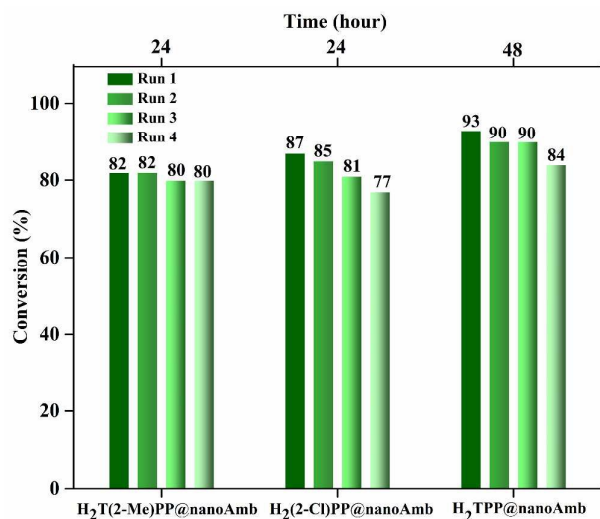


Figure 7. Catalyst reusability of H₂TPP@nanoAmb under the optimized reaction conditions.

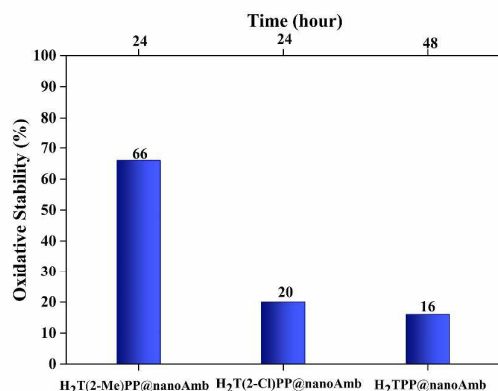


Figure 8. The catalyst stability after four successive reuse cycles.

It should be noted that the Soret band of H₂TPP(HCl)₂ should appear at ca. 442 nm. Accordingly, the acid immobilized catalyst is stable towards anion exchange with HCl. In a previous study, we demonstrated that the anion exchange with a porphyrin dication requires decomposition of the dication into free base porphyrin^[47].

Oxidation of cyclohexene

The photooxidation of cyclohexene was also conducted using the Amb supported porphyrins (Table 6). Herein, allylic ketone was obtained as the main product. In contrast to the oxidation of cyclooctene (Table 5), running the oxidation of cyclohexene in the presence of sun light led to a remarkable increase in the rate of the reaction; it is observed that the TOF values are ca. two times than those obtained in the case the 20 W white LED lamps. The oxidation was also performed under sun light.

Herein, the reaction times were much shorter than those in the presence of the LED lamps. It should be noted that the change of

light source in the oxidation of cyclooctene led to little changes in the reaction rate. The comparison of the data summarized in (Tables 5) shows higher reactivity of cyclooctene than cyclohexene.

Reactive oxygen species

The involvement of singlet oxygen and/or superoxide anion radical species in the aerobic oxidation of organic compounds^[9,44] catalyzed by free base porphyrins and H₂TPP(DDQ)₂ was evident in previous studies^[45]. 1,3-diphenylisobenzofuran (DPBF) as a well known singlet oxygen scavenger was used to determine^[48-50] the reactive oxygen species responsible for the oxidation of cyclooctene. A solution of DPBF in acetonitrile (5 × 10⁻⁵ M) was irradiated with a 10 W red LED lamp for 10 min prior to the addition of the photosensitizer.

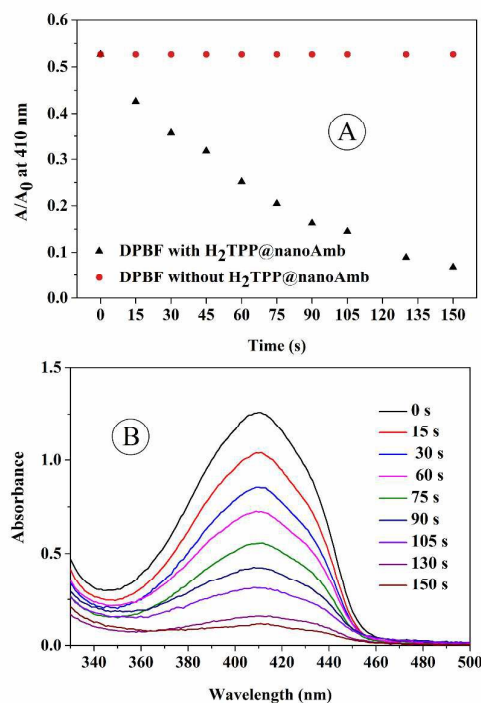


Figure 9. (a) The variation in the absorbance at the λ_{max} of DPBF versus time in the absence and presence of H₂TPP@nanoAmb. (b) The spectral changes at the λ_{max} of DPBF after exposure to a 10 W red LED lamp in presence of the photosensitizer.

Table 6. Photooxidation of cyclohexene.

Photosensitizers	White LED			Sun Light		
	Time (h)	Conversion (Oxidative stability) (%)	TON [TOF (h ⁻¹)]	Time (h)	Conversion (Oxidative stability) (%)	TON [TOF (h ⁻¹)]
H ₂ TPP@nanoAmb	48	89 (60)	8900 [185]	24	90 [51]	9000 [375]
H ₂ T(2-Cl)PP@nanoAmb	48	95 (61)	9500 [198]	24	92 [65]	9200 [383]
H ₂ T(2-Me)PP@nanoAmb	48	80 (88)	8000 [167]	24	68 [90]	6800 [283]

^a Catalyst and cyclohexene were used in 1:10000 molar ratio in acetonitrile. 2-cyclohexene-1-one was the major product (Supporting Information, S3). See the footnotes of Table 3 for more details.

No detectable changes were observed in the intensity of the absorption band at 410 nm. The addition of H₂TPP@nanoAmb led to gradual decrease in the absorbance at 410 nm (Figure 9) that provides considerable evidence for the involvement of singlet oxygen as the major ROS. On the other hand, the oxidation of cyclooctene was conducted in the presence of 1,4-benzoquinone (in 1:2 molar ratio relative to cyclooctene) as a superoxide anion radical scavenger^[51-52] and no change in the yield of the oxidation product was observed. It should be noted that the order of photocatalytic activity of the catalyst in different solvents was also in a good agreement with the lifetime of singlet oxygen in these solvents.

Conclusion

A series of meso-tetra(aryl)porphyrins supported on Amberlyst 15 nanoparticles via acid base reaction were used as highly efficient heterogeneous photocatalysts (TON values in the range of 8000-10000) for the aerobic oxidation of olefins and found that: (i) The polymer nanoparticles with an average diameter less than 200 nm can be readily synthesized by stirring the polymer beads in ethyl acetate for 24 h; (ii) the concomitant protonation and immobilization of porphyrins led to a significant increase in the oxidative stability of porphyrins with respect to their non-immobilized counterparts so that the porphyrins may be recovered and reused at least four times without significant decrease in their catalytic activity; (iii) the very limited solubility or insolubility of porphyrins in acetonitrile that is a disadvantage in homogeneous photocatalysis of oxidation reactions catalyzed by non-metallated porphyrins was used as an advantage to design a heterogeneous catalytic system with no-catalyst leaching over long reaction times; (iv) porphyrin dications may be prepared in safe, non-toxic and eco-friendly solvents. Also, the loaded porphyrin may be readily separated from the polymer by a simple alkaline treatment and measured by UV-vis spectroscopy. Furthermore, the polymer can be recovered and reused after an acid treatment; (v) with the exception of some highly electron-deficient porphyrins, all previously synthesized porphyrins may be readily immobilized on Amberlyst-15 nanoparticles as a strong acid to form a large library of heterogeneous porphyrinic photosensitizers; (vi) interestingly, the maximum catalyst performance was observed in the presence of a remarkably low degree of porphyrin loading; (vii) the highest oxidative stability and catalytic activity were observed in the

case of H₂T(2-Me)PP@nanoAmb and H₂T(2-Cl)PP@nanoAmb, respectively.

Acknowledgements

Financial support of this work by Institute for Advanced Studies in Basic Sciences (IASBS) is acknowledged.

References

- [1] R. Bonnett, *Chem. Soc. Rev.* 1995, **24**, 19-33.
- [2] M. Klaper, W. Fudickar and T. Linker, *J. Am. Chem. Soc.* 2016, **138**, 7024-7029.
- [3] E. Secret, M. Maynadier, A. Gallud, M. Gary-Bobo, A. Chaix, E. Belamie, P. Maillard, M. J. Sailor, M. Garcia, J.-O. Durand and F. Cunin, *Chem. Commun.* 2013, **49**, 4202-4204.
- [4] H. Liu, W. Feng, C. W. Kee, Y. Zhao, D. Leow, Y. Pan and C.H. Tan, *Green Chem.* 2010, **12**, 953-956.
- [5] D. Topkaya, D. Lafont, F. Poyer, G. Garcia, F. Albrieux, P. Maillard, Y. Bretonnière and F. Dumoulin, *New J. Chem.* 2016, **40**, 2044-2050.
- [6] X.-H. Dai, Z.-M. Wang, L.-Y. Gao, J.-M. Pan, X.-H. Wang, Yong-S. Yan and D.-M. Liu, *New J. Chem.* 2014, **38**, 3569-3578.
- [7] P. R. Ogilby, *Chem. Soc. Rev.* 2010, **39**, 3181-3209.
- [8] M. C. DeRosa and R. J. Crutchley, *Coord. Chem. Rev.* 2002, **233**, 351-371.
- [9] Ana M. Perez-Lopez, Elsa Valero and Mark Bradley, *New J. Chem.* 2017, In press.
- [10] M. Pineiro, A. L. Carvalho, M. M. Pereira, A. d. A. Gonsalves, L. G. Arnaut and S. J. Formosinho, *Chem. Eur. J.* 1998, **4**, 2299-2307.
- [11] D. Yao, V. Hugues, M. Blanchard-Desce, O. Mongin, C. O. Paul-Roth and F. Paul, *New J. Chem.* 2015, **39**, 7730-7733.
- [12] S. Campestrini and U. Tonellato, *Eur. J. Org. Chem.* 2002, **22**, 3827-3832.
- [13] S. Zakavi and S. Hoseini, *RSC Adv.* 2015, **5**, 106774-106786;
- [14] A. Rosa, G. Ricciardi, E. J. Baerends, A. Romeo and L. Monsù Scolaro, *J. Phys. Chem. A* 2003, **107**, 11468-11482.
- [15] H. H. Thanga and A. L. Verma, *New J. Chem.*, 2002, **26**, 342-346.
- [16] N. E. Leadbeater and M. Marco, *Chem. Soc. Rev.* 2002, **102**, 3217-3274.
- [17] S. M. Ribeiro, A. C. Serra and A. d. A. R. Gonsalves, *Tetrahedron* 2007, **63**, 7885-7891.
- [18] J. Bhaumik, G. Gogia, S. Kirar, L. Vijay, N. S. Thakur, U. C. Banerjee and J. K. Laha, *New J. Chem.* 2016, **40**, 724-731.
- [19] K. Teramura, H. Tsuneoka, K. Ogura, T. Sugimoto, T. Shishido and T. Tanaka, *ChemCatChem* 2014, **6**, 2276-2281.
- [20] E. Brule and Y. R. de Miguel, *Org. Biomol. Chem.* 2006, **4**, 599-609.
- [21] L. Fernández, V. I. Esteves, Â. Cunha, R. J. Schneider and J. P. Tomé, *J. Porphyrins Phthalocyanines* 2016, **20**, 150-166.

- [22] D. Murtinho, M. Pineiro, M. M. Pereira, A. M. d. A. R. Gonsalves, L. G. Arnaut, M. da Graça Miguel and H. D. Burrows, *J. Chem. Soc., Perkin Trans. 2*, 2000, 2441–2447.
- [23] J. Johnson Inbaraj, M. V. Vinodu, R. Gandhidasan, R. Murugesan and M. Padmanabhan, *J. Appl. Polym. Sci.* 2003, **89**, 3925–3930.
- [24] P. Henke, K. Lang, P. Kubát, J. Sýkora, M. Šlouf and J. í. Mosinger, *ACS Appl. Mater. Interfaces* 2013, **5**, 3776–3783.
- [25] J. Suchánek, P. Henke, J. í. Mosinger, Z. k. Zelinger and P. Kubát, *J. Phys. Chem. B*. 2014, **118**, 6167–6174.
- [26] S. Ribeiro, A. C. Serra and A. R. Gonsalves, *ChemCatChem* 2013, **5**, 134–137.
- [27] M. Meot-Ner, A. D. Adler, *J. Am. Chem. Soc.* 1975, **97**, 5107–5111.
- [28] S. Zakavi, R. Omidyan and S. Talebzadeh, *RSC Adv.* 2016, **6**, 82219–82226.
- [29] B. Cheng, O. Q. Munro, H. M. Marques and W. R. Scheidt, *J. Am. Chem. Soc.* 1997, **119**, 10732–10742.
- [30] J. Yadav, B. Reddy, B. Eshwaraiah and K. Anuradha, *Green Chem.* 2002, **4**, 592–594.
- [31] M. Rezayat and H. S. Ghaziaskar, *Green Chem.* 2009, **11**, 710–715.
- [32] Z. Amara, J. F. Bellamy, R. Horvath, S. J. Miller, A. Beeby, A. Burgard, K. Rossen, M. Poliakoff and M. W. George, *Nat. Chem.* 2015, **7**, 489–495.
- [33] G. Dyrda, R. Słota, M. A. Broda and G. Mele, *Res. Chem. Intermed.* 2016, **42**, 3789–3804.
- [34] E. Safaei, S. Mohebbi, *J. Mater. Chem. A* 2016, **4**, 3933–3946.
- [35] A. D. Adler, F. R. Longo, J. D. Finarelli, J. Goldmacher, J. Assour and L. Korsakoff, *J. Org. Chem.* 1967, **32**, 476–476.
- [36] A. Stone and E. B. Fleischer, *J. Am. Chem. Soc.* 1968, **90**, 2735–2748.
- [36] S. Zakavi and N. G. Gharab, *Polyhedron* 2007, **26**, 2425–2432.
- [37] L. Wang and F.-S. Xiao, *Green Chem.* 2015, **17**, 24–39.
- [38] T. A. Peters, N. E. Benes, A. Holmen and J. T. Keurentjes, *Appl. Catal. A* 2006, **297**, 182–188.
- [39] X. Ding and B. H. Han, *Angew. Chem. Int. Ed. Engl.* 2015, **54**, 6536–6539.
- [40] J. Hynek, J. Rathouský, J. Demel and K. Lang, *RSC Adv.* 2016, **6**, 44279–44287.
- [41] A. Ogunsipe, J.-Y. Chen, T. Nyokong, *New J. Chem.* 2004, **28**, 822–827.
- [42] M. Bregnhøj, M. Westberg, F. Jensen and P. R. Ogilby, *Phys. Chem. Chem. Phys.* 2016, **18**, 22946–22961.
- [43] Y. Chen, S. Xu, L. Li, M. Zhang, J. Shen and T. Shen, *Dyes Pigments* 2001, **51**, 63–69.
- [44] I. Kruk, H. Y. Aboul - Enein, T. Michalska, K. Lichszteld, K. Kubasik - Kladna and S. Ölgen, *Luminescence* 2007, **22**, 379–386.
- [45] A. G. Mojjarrad and S. Zakavi, *RSC Adv.* 2016, **6**, 100931–100938.
- [46] L. Pauling, *The nature of the chemical bond and the structure of molecules and crystals, Vol. 18*, Cornell university press, 1960.
- [47] S. Zakavi, H. Rahiminezhad and R. Alizadeh, *Spectrochimica Acta Part A* 2010, **77**, 994–997.
- [48] M. A. Caine, R. W. McCabe, L. Wang, R. G. Brown, J. D. Hepworth, *Dyes Pigments* 2001, **49**, 135–143.
- [49] J. Park, D. Feng, S. Yuan and H. C. Zhou, *Angew. Chem. Int. Ed. Engl.* 2015, **54**, 430–435.
- [50] E. Gürel, M. Pişkin, S. Altun, Z. Odabaş and M. Durmuş, *Dalton Trans.* 2015, **44**, 6202–6211.
- [51] M. I. Gutiérrez, *Photochem. Photobiol. Sci.* 2008, **7**, 480–484;
- [52] A. Casado-Sánchez, R. Gómez-Ballesteros, F. Tato, F. J. Soriano, G. Pascual-Coca, S. Cabrera and J. Alemán, *Chem. Commun.* 2016, **52**, 9137–9140.